

Search for a light Higgs boson decaying to two gluons or $s\bar{s}$ in the radiative decays of $\Upsilon(1S)$

J. P. Lees,¹ V. Poireau,¹ V. Tisserand,¹ E. Grauges,² A. Palano^{ab,3} G. Eigen,⁴ B. Stugu,⁴ D. N. Brown,⁵ L. T. Kerth,⁵ Yu. G. Kolomensky,⁵ M. J. Lee,⁵ G. Lynch,⁵ H. Koch,⁶ T. Schroeder,⁶ C. Hearty,⁷ T. S. Mattison,⁷ J. A. McKenna,⁷ R. Y. So,⁷ A. Khan,⁸ V. E. Blinov^{ac,9} A. R. Buzykaev^{a,9} V. P. Druzhinin^{ab,9} V. B. Golubev^{ab,9} E. A. Kravchenko^{ab,9} A. P. Onuchin^{ac,9} S. I. Serednyakov^{ab,9} Yu. I. Skovpen^{ab,9} E. P. Solodov^{ab,9} K. Yu. Todyshev^{ab,9} A. N. Yushkov^{a,9} D. Kirkby,¹⁰ A. J. Lankford,¹⁰ M. Mandelkern,¹⁰ B. Dey,¹¹ J. W. Gary,¹¹ O. Long,¹¹ G. M. Vitug,¹¹ C. Campagnari,¹² M. Franco Sevilla,¹² T. M. Hong,¹² D. Kovalskyi,¹² J. D. Richman,¹² C. A. West,¹² A. M. Eisner,¹³ W. S. Lockman,¹³ B. A. Schumm,¹³ A. Seiden,¹³ D. S. Chao,¹⁴ C. H. Cheng,¹⁴ B. Echenard,¹⁴ K. T. Flood,¹⁴ D. G. Hitlin,¹⁴ P. Ongmongkolkul,¹⁴ F. C. Porter,¹⁴ R. Andreassen,¹⁵ Z. Huard,¹⁵ B. T. Meadows,¹⁵ B. G. Pushpawela,¹⁵ M. D. Sokoloff,¹⁵ L. Sun,¹⁵ P. C. Bloom,¹⁶ W. T. Ford,¹⁶ A. Gaz,¹⁶ U. Nauenberg,¹⁶ J. G. Smith,¹⁶ S. R. Wagner,¹⁶ R. Ayad,^{17,*} W. H. Toki,¹⁷ B. Spaan,¹⁸ R. Schwierz,¹⁹ D. Bernard,²⁰ M. Verderi,²⁰ S. Playfer,²¹ D. Bettoni^{a,22} C. Bozzi^{a,22} R. Calabrese^{ab,22} G. Cibinetto^{ab,22} E. Fioravanti^{ab,22} I. Garzia^{ab,22} E. Luppi^{ab,22} L. Piemontese^{a,22} V. Santoro^{a,22} R. Baldini-Ferrolli,²³ A. Calcaterra,²³ R. de Sangro,²³ G. Finocchiaro,²³ S. Martellotti,²³ P. Patteri,²³ I. M. Peruzzi,^{23,†} M. Piccolo,²³ M. Rama,²³ A. Zallo,²³ R. Contri^{ab,24} E. Guido^{ab,24} M. Lo Vetere^{ab,24} M. R. Monge^{ab,24} S. Passaggio^{a,24} C. Patrignani^{ab,24} E. Robutti^{a,24} B. Bhuyan,²⁵ V. Prasad,²⁵ M. Morii,²⁶ A. Adametz,²⁷ U. Uwer,²⁷ H. M. Lacker,²⁸ P. D. Dauncey,²⁹ U. Mallik,³⁰ C. Chen,³¹ J. Cochran,³¹ W. T. Meyer,³¹ S. Prell,³¹ A. V. Gritsan,³² N. Arnaud,³³ M. Davier,³³ D. Derkach,³³ G. Grosdidier,³³ F. Le Diberder,³³ A. M. Lutz,³³ B. Malaescu,^{33,‡} P. Roudeau,³³ A. Stocchi,³³ G. Wormser,³³ D. J. Lange,³⁴ D. M. Wright,³⁴ J. P. Coleman,³⁵ J. R. Fry,³⁵ E. Gabathuler,³⁵ D. E. Hutchcroft,³⁵ D. J. Payne,³⁵ C. Touramanis,³⁵ A. J. Bevan,³⁶ F. Di Lodovico,³⁶ R. Sacco,³⁶ G. Cowan,³⁷ J. Bougher,³⁸ D. N. Brown,³⁸ C. L. Davis,³⁸ A. G. Denig,³⁹ M. Fritsch,³⁹ W. Gradl,³⁹ K. Griessinger,³⁹ A. Hafner,³⁹ E. Prencipe,³⁹ K. Schubert,³⁹ R. J. Barlow,^{40,§} G. D. Lafferty,⁴⁰ E. Behn,⁴¹ R. Cenci,⁴¹ B. Hamilton,⁴¹ A. Jawahery,⁴¹ D. A. Roberts,⁴¹ R. Cowan,⁴² D. Dujmic,⁴² G. Sciolla,⁴² R. Cheaib,⁴³ P. M. Patel,^{43,¶} S. H. Robertson,⁴³ P. Biassoni^{ab,44} N. Neri^{a,44} F. Palombo^{ab,44} L. Cremaldi,⁴⁵ R. Godang,^{45,**} P. Sonnek,⁴⁵ D. J. Summers,⁴⁵ M. Simard,⁴⁶ P. Taras,⁴⁶ G. De Nardo^{ab,47} D. Monorchio^{ab,47} G. Onorato^{ab,47} C. Sciacca^{ab,47} M. Martinelli,⁴⁸ G. Raven,⁴⁸ C. P. Jessop,⁴⁹ J. M. LoSecco,⁴⁹ K. Honscheid,⁵⁰ R. Kass,⁵⁰ J. Brau,⁵¹ R. Frey,⁵¹ N. B. Sinev,⁵¹ D. Strom,⁵¹ E. Torrence,⁵¹ E. Feltres^{ab,52} M. Margoni^{ab,52} M. Morandin^{a,52} M. Posocco^{a,52} M. Rotondo^{a,52} G. Simi^{a,52} F. Simonetto^{ab,52} R. Stroili^{ab,52} S. Akar,⁵³ E. Ben-Haim,⁵³ M. Bomben,⁵³ G. R. Bonneaud,⁵³ H. Briand,⁵³ G. Calderini,⁵³ J. Chauveau,⁵³ Ph. Leruste,⁵³ G. Marchiori,⁵³ J. Ocariz,⁵³ S. Sitt,⁵³ M. Biasini^{ab,54} E. Manoni^{a,54} S. Pacetti^{ab,54} A. Rossi^{a,54} C. Angelini^{ab,55} G. Batignani^{ab,55} S. Bettarini^{ab,55} M. Carpinelli^{ab,55,††} G. Casarosa^{ab,55} A. Cervelli^{ab,55} F. Forti^{ab,55} M. A. Giorgi^{ab,55} A. Lusiani^{ac,55} B. Oberhof^{ab,55} E. Paoloni^{ab,55} A. Perez^{a,55} G. Rizzo^{ab,55} J. J. Walsh^{a,55} D. Lopes Pegna,⁵⁶ J. Olsen,⁵⁶ A. J. S. Smith,⁵⁶ R. Faccini^{ab,57} F. Ferrarotto^{a,57} F. Ferroni^{ab,57} M. Gaspero^{ab,57} L. Li Gioi^{a,57} G. Piredda^{a,57} C. Büniger,⁵⁸ O. Grünberg,⁵⁸ T. Hartmann,⁵⁸ T. Leddig,⁵⁸ C. Voß,⁵⁸ R. Waldi,⁵⁸ T. Adye,⁵⁹ E. O. Olaiya,⁵⁹ F. F. Wilson,⁵⁹ S. Emery,⁶⁰ G. Hamel de Monchenault,⁶⁰ G. Vasseur,⁶⁰ Ch. Yèche,⁶⁰ F. Anulli,^{61,‡‡} D. Aston,⁶¹ D. J. Bard,⁶¹ J. F. Benitez,⁶¹ C. Cartaro,⁶¹ M. R. Convery,⁶¹ J. Dorfan,⁶¹ G. P. Dubois-Felsmann,⁶¹ W. Dunwoodie,⁶¹ M. Ebert,⁶¹ R. C. Field,⁶¹ B. G. Fulsom,⁶¹ A. M. Gabareen,⁶¹ M. T. Graham,⁶¹ C. Hast,⁶¹ W. R. Innes,⁶¹ P. Kim,⁶¹ M. L. Kocian,⁶¹ D. W. G. S. Leith,⁶¹ P. Lewis,⁶¹ D. Lindemann,⁶¹ B. Lindquist,⁶¹ S. Luitz,⁶¹ V. Luth,⁶¹ H. L. Lynch,⁶¹ D. B. MacFarlane,⁶¹ D. R. Muller,⁶¹ H. Neal,⁶¹ S. Nelson,⁶¹ M. Perl,⁶¹ T. Pulliam,⁶¹ B. N. Ratcliff,⁶¹ A. Roodman,⁶¹ A. A. Salnikov,⁶¹ R. H. Schindler,⁶¹ A. Snyder,⁶¹ D. Su,⁶¹ M. K. Sullivan,⁶¹ J. Va'vra,⁶¹ A. P. Wagner,⁶¹ W. F. Wang,⁶¹ W. J. Wisniewski,⁶¹ M. Wittgen,⁶¹ D. H. Wright,⁶¹ H. W. Wulsin,⁶¹ V. Ziegler,⁶¹ W. Park,⁶² M. V. Purohit,⁶² R. M. White,^{62,§§} J. R. Wilson,⁶² A. Randle-Conde,⁶³ S. J. Sekula,⁶³ M. Bellis,⁶⁴ P. R. Burchat,⁶⁴ T. S. Miyashita,⁶⁴ E. M. T. Puccio,⁶⁴ M. S. Alam,⁶⁵ J. A. Ernst,⁶⁵ R. Gorodeisky,⁶⁶ N. Guttman,⁶⁶ D. R. Peimer,⁶⁶ A. Soffer,⁶⁶ S. M. Spanier,⁶⁷ J. L. Ritchie,⁶⁸ A. M. Ruland,⁶⁸ R. F. Schwitters,⁶⁸ B. C. Wray,⁶⁸ J. M. Izen,⁶⁹ X. C. Lou,⁶⁹ F. Bianchi^{ab,70} F. De Mori^{ab,70} A. Filippi^{a,70} D. Gamba^{ab,70} S. Zambito^{ab,70} L. Lanceri^{ab,71} L. Vitale^{ab,71} F. Martinez-Vidal,⁷² A. Oyanguren,⁷² P. Villanueva-Perez,⁷²

H. Ahmed,⁷³ J. Albert,⁷³ Sw. Banerjee,⁷³ F. U. Bernlochner,⁷³ H. H. F. Choi,⁷³ G. J. King,⁷³ R. Kowalewski,⁷³
M. J. Lewczuk,⁷³ T. Lueck,⁷³ I. M. Nugent,⁷³ J. M. Roney,⁷³ R. J. Sobie,⁷³ N. Tasneem,⁷³ T. J. Gershon,⁷⁴
P. F. Harrison,⁷⁴ T. E. Latham,⁷⁴ H. R. Band,⁷⁵ S. Dasu,⁷⁵ Y. Pan,⁷⁵ R. Prepost,⁷⁵ and S. L. Wu⁷⁵

(The BABAR Collaboration)

¹Laboratoire d'Annecy-le-Vieux de Physique des Particules (LAPP),
Université de Savoie, CNRS/IN2P3, F-74941 Annecy-Le-Vieux, France

²Universitat de Barcelona, Facultat de Física, Departament ECM, E-08028 Barcelona, Spain

³INFN Sezione di Bari^a; Dipartimento di Fisica, Università di Bari^b, I-70126 Bari, Italy

⁴University of Bergen, Institute of Physics, N-5007 Bergen, Norway

⁵Lawrence Berkeley National Laboratory and University of California, Berkeley, California 94720, USA

⁶Ruhr Universität Bochum, Institut für Experimentalphysik 1, D-44780 Bochum, Germany

⁷University of British Columbia, Vancouver, British Columbia, Canada V6T 1Z1

⁸Brunel University, Uxbridge, Middlesex UB8 3PH, United Kingdom

⁹Budker Institute of Nuclear Physics SB RAS, Novosibirsk 630090^a,
Novosibirsk State University, Novosibirsk 630090^b,

Novosibirsk State Technical University, Novosibirsk 630092^c, Russia

¹⁰University of California at Irvine, Irvine, California 92697, USA

¹¹University of California at Riverside, Riverside, California 92521, USA

¹²University of California at Santa Barbara, Santa Barbara, California 93106, USA

¹³University of California at Santa Cruz, Institute for Particle Physics, Santa Cruz, California 95064, USA

¹⁴California Institute of Technology, Pasadena, California 91125, USA

¹⁵University of Cincinnati, Cincinnati, Ohio 45221, USA

¹⁶University of Colorado, Boulder, Colorado 80309, USA

¹⁷Colorado State University, Fort Collins, Colorado 80523, USA

¹⁸Technische Universität Dortmund, Fakultät Physik, D-44221 Dortmund, Germany

¹⁹Technische Universität Dresden, Institut für Kern- und Teilchenphysik, D-01062 Dresden, Germany

²⁰Laboratoire Leprince-Ringuet, Ecole Polytechnique, CNRS/IN2P3, F-91128 Palaiseau, France

²¹University of Edinburgh, Edinburgh EH9 3JZ, United Kingdom

²²INFN Sezione di Ferrara^a; Dipartimento di Fisica e Scienze della Terra, Università di Ferrara^b, I-44122 Ferrara, Italy

²³INFN Laboratori Nazionali di Frascati, I-00044 Frascati, Italy

²⁴INFN Sezione di Genova^a; Dipartimento di Fisica, Università di Genova^b, I-16146 Genova, Italy

²⁵Indian Institute of Technology Guwahati, Guwahati, Assam, 781 039, India

²⁶Harvard University, Cambridge, Massachusetts 02138, USA

²⁷Universität Heidelberg, Physikalisches Institut, D-69120 Heidelberg, Germany

²⁸Humboldt-Universität zu Berlin, Institut für Physik, D-12489 Berlin, Germany

²⁹Imperial College London, London, SW7 2AZ, United Kingdom

³⁰University of Iowa, Iowa City, Iowa 52242, USA

³¹Iowa State University, Ames, Iowa 50011-3160, USA

³²Johns Hopkins University, Baltimore, Maryland 21218, USA

³³Laboratoire de l'Accélérateur Linéaire, IN2P3/CNRS et Université Paris-Sud 11,
Centre Scientifique d'Orsay, F-91898 Orsay Cedex, France

³⁴Lawrence Livermore National Laboratory, Livermore, California 94550, USA

³⁵University of Liverpool, Liverpool L69 7ZE, United Kingdom

³⁶Queen Mary, University of London, London, E1 4NS, United Kingdom

³⁷University of London, Royal Holloway and Bedford New College, Egham, Surrey TW20 0EX, United Kingdom

³⁸University of Louisville, Louisville, Kentucky 40292, USA

³⁹Johannes Gutenberg-Universität Mainz, Institut für Kernphysik, D-55099 Mainz, Germany

⁴⁰University of Manchester, Manchester M13 9PL, United Kingdom

⁴¹University of Maryland, College Park, Maryland 20742, USA

⁴²Massachusetts Institute of Technology, Laboratory for Nuclear Science, Cambridge, Massachusetts 02139, USA

⁴³McGill University, Montréal, Québec, Canada H3A 2T8

⁴⁴INFN Sezione di Milano^a; Dipartimento di Fisica, Università di Milano^b, I-20133 Milano, Italy

⁴⁵University of Mississippi, University, Mississippi 38677, USA

⁴⁶Université de Montréal, Physique des Particules, Montréal, Québec, Canada H3C 3J7

⁴⁷INFN Sezione di Napoli^a; Dipartimento di Scienze Fisiche,
Università di Napoli Federico II^b, I-80126 Napoli, Italy

⁴⁸NIKHEF, National Institute for Nuclear Physics and High Energy Physics, NL-1009 DB Amsterdam, The Netherlands

⁴⁹University of Notre Dame, Notre Dame, Indiana 46556, USA

⁵⁰Ohio State University, Columbus, Ohio 43210, USA

⁵¹University of Oregon, Eugene, Oregon 97403, USA

⁵²INFN Sezione di Padova^a; Dipartimento di Fisica, Università di Padova^b, I-35131 Padova, Italy

- ⁵³Laboratoire de Physique Nucléaire et de Hautes Energies,
IN2P3/CNRS, Université Pierre et Marie Curie-Paris6,
Université Denis Diderot-Paris7, F-75252 Paris, France
- ⁵⁴INFN Sezione di Perugia^a; Dipartimento di Fisica, Università di Perugia^b, I-06123 Perugia, Italy
- ⁵⁵INFN Sezione di Pisa^a; Dipartimento di Fisica,
Università di Pisa^b; Scuola Normale Superiore di Pisa^c, I-56127 Pisa, Italy
- ⁵⁶Princeton University, Princeton, New Jersey 08544, USA
- ⁵⁷INFN Sezione di Roma^a; Dipartimento di Fisica,
Università di Roma La Sapienza^b, I-00185 Roma, Italy
- ⁵⁸Universität Rostock, D-18051 Rostock, Germany
- ⁵⁹Rutherford Appleton Laboratory, Chilton, Didcot, Oxon, OX11 0QX, United Kingdom
- ⁶⁰CEA, Irfu, SPP, Centre de Saclay, F-91191 Gif-sur-Yvette, France
- ⁶¹SLAC National Accelerator Laboratory, Stanford, California 94309 USA
- ⁶²University of South Carolina, Columbia, South Carolina 29208, USA
- ⁶³Southern Methodist University, Dallas, Texas 75275, USA
- ⁶⁴Stanford University, Stanford, California 94305-4060, USA
- ⁶⁵State University of New York, Albany, New York 12222, USA
- ⁶⁶Tel Aviv University, School of Physics and Astronomy, Tel Aviv, 69978, Israel
- ⁶⁷University of Tennessee, Knoxville, Tennessee 37996, USA
- ⁶⁸University of Texas at Austin, Austin, Texas 78712, USA
- ⁶⁹University of Texas at Dallas, Richardson, Texas 75083, USA
- ⁷⁰INFN Sezione di Torino^a; Dipartimento di Fisica, Università di Torino^b, I-10125 Torino, Italy
- ⁷¹INFN Sezione di Trieste^a; Dipartimento di Fisica, Università di Trieste^b, I-34127 Trieste, Italy
- ⁷²IFIC, Universitat de Valencia-CSIC, E-46071 Valencia, Spain
- ⁷³University of Victoria, Victoria, British Columbia, Canada V8W 3P6
- ⁷⁴Department of Physics, University of Warwick, Coventry CV4 7AL, United Kingdom
- ⁷⁵University of Wisconsin, Madison, Wisconsin 53706, USA

We search for the decay $\Upsilon(1S) \rightarrow \gamma A^0, A^0 \rightarrow gg$ or $s\bar{s}$, where A^0 is the pseudoscalar light Higgs boson predicted by the next-to-minimal supersymmetric standard model. We use a sample of $(17.6 \pm 0.3) \times 10^6$ $\Upsilon(1S)$ mesons produced in the BABAR experiment via $e^+e^- \rightarrow \Upsilon(2S) \rightarrow \pi^+\pi^-\Upsilon(1S)$. We see no significant signal and set 90%-confidence-level upper limits on the product branching fraction $\mathcal{B}(\Upsilon(1S) \rightarrow \gamma A^0) \cdot \mathcal{B}(A^0 \rightarrow gg \text{ or } s\bar{s})$ ranging from 10^{-6} to 10^{-2} for A^0 masses in the range 0.5 to 9.0 GeV/ c^2 .

PACS numbers: 14.80.Da, 14.40.Pq, 13.20.Gd, 12.60.Fr, 12.15.Ji

The next-to-minimal supersymmetric standard model (NMSSM), one of several extensions to the Standard Model [1], predicts that there are two charged, three neutral CP -even, and two neutral CP -odd Higgs bosons. One of the CP -odd Higgs bosons, A^0 , can be lighter than two bottom quarks [2]. If so, a CP -odd Higgs boson that couples to bottom quarks could be produced in the radiative decays of an Υ meson.

The A^0 is a superposition of a singlet and a non-singlet

state. The branching fraction $\mathcal{B}(\Upsilon \rightarrow \gamma A^0)$ depends on the NMSSM parameter $\cos\theta_A$, which is the non-singlet fraction. The final state to which the A^0 decays depends on various parameters such as $\tan\beta$ and the A^0 mass [3]. BABAR has searched for an A^0 decaying into $\mu^+\mu^-$ [4, 5], $\tau^+\tau^-$ [6, 7], invisible states [8], and hadronic final states [9], and has not seen a significant signal. The CMS collaboration has also not observed a significant signal in the search for A^0 decaying into $\mu^+\mu^-$ [10]. In this article, we report on the first search for the decay $\Upsilon(1S) \rightarrow \gamma A^0, A^0 \rightarrow gg$ or $s\bar{s}$. We search for the A^0 in the mass range $0.5 < m_{A^0} < 9.0$ GeV/ c^2 . By tagging the dipion in the $\Upsilon(2S) \rightarrow \pi^+\pi^-\Upsilon(1S)$ transition, this analysis greatly reduces $e^+e^- \rightarrow q\bar{q}$ background, where q is a u, d , or s quark, which is a dominant background contribution in BABAR's previous $A^0 \rightarrow$ hadrons analysis [9]. Although this analysis has been motivated by NMSSM, these results are generally applicable to any CP -odd hadronic resonances produced in the radiative decays of $\Upsilon(1S)$ because we search for the A^0 excluding two-body final states. For an A^0 mass less than $2m_\tau$, the A^0 is predicted to decay predominantly into two gluons if $\tan\beta$ is of order 1, and into $s\bar{s}$ if $\tan\beta$ is of order 10.

This article uses data recorded with the BABAR detec-

*Now at the University of Tabuk, Tabuk 71491, Saudi Arabia

†Also with Università di Perugia, Dipartimento di Fisica, Perugia, Italy

‡Also with Laboratoire de Physique Nucléaire et de Hautes Energies, IN2P3/CNRS, Paris, France

§Now at the University of Huddersfield, Huddersfield HD1 3DH, UK

¶Deceased

**Now at University of South Alabama, Mobile, Alabama 36688, USA

††Also with Università di Sassari, Sassari, Italy

‡‡Also with INFN Sezione di Roma, Roma, Italy

§§Now at Universidad Técnica Federico Santa María, Valparaíso, Chile 2390123

tor at the PEP-II asymmetric-energy e^+e^- collider at the SLAC National Accelerator Laboratory. The *BABAR* detector is described in detail elsewhere [11, 12]. For this analysis, we use 13.6fb^{-1} of data [13] taken at the $\Upsilon(2S)$ resonance (“on-resonance”). An estimated number of $(98.3 \pm 0.9) \times 10^6$ $\Upsilon(2S)$ mesons were produced. The branching fraction $\mathcal{B}(\Upsilon(2S) \rightarrow \pi^+\pi^-\Upsilon(1S))$ is $(17.92 \pm 0.26)\%$ [14]. Therefore, $(17.6 \pm 0.3) \times 10^6$ $\Upsilon(1S)$ mesons were produced via the dipion transition. We also use 1.4fb^{-1} of data [13] taken 30 MeV below the $\Upsilon(2S)$ resonance (“off-resonance”) as a background sample.

Simulated signal events with various A^0 masses ranging from 0.5 to 9.0 GeV/c^2 are used in this analysis. The *EvtGen* event generator [15] is used to simulate particle decays. The A^0 is simulated as a spin-0 particle decaying to either gg or $s\bar{s}$. Since the width of the A^0 is expected to be much less than the invariant-mass resolution of $\approx 100\text{MeV}/c^2$, we simulate the A^0 with a $1\text{MeV}/c^2$ decay width. *Jetset* [16] is used to hadronize partons, and *GEANT4* [17] is used to simulate the detector response.

We select events with two charged tracks as the dipion system candidate, a radiative photon, and a hadronic system, as described later in this article. We select $\Upsilon(2S) \rightarrow \pi^+\pi^-\Upsilon(1S)$ candidates based on the invariant mass m_R of the system recoiling against the dipion system:

$$m_R^2 = M_{\Upsilon(2S)}^2 + m_{\pi\pi}^2 - 2M_{\Upsilon(2S)}E_{\pi\pi}^{CM}, \quad (1)$$

where $M_{\Upsilon(2S)}$ is the world average $\Upsilon(2S)$ mass [14], $m_{\pi\pi}$ is the measured dipion invariant mass, and $E_{\pi\pi}^{CM}$ is the dipion energy in the e^+e^- center-of-mass (CM) frame. The recoil mass distribution from an $\Upsilon(2S) \rightarrow \pi^+\pi^-\Upsilon(1S)$ transition has a peak near the $\Upsilon(1S)$ mass of $9.46030 \pm 0.00026\text{GeV}/c^2$ [14]. The background recoil mass distribution is uniform. We select events with a recoil mass in the range 9.45 to 9.47 GeV/c^2 . We further suppress the background with a multi-layer perceptron (MLP) neural network [18]. Using simulated $\Upsilon(2S) \rightarrow \pi^+\pi^-\Upsilon(1S)$, $\Upsilon(1S) \rightarrow \gamma A^0$ decays of various A^0 masses, $\Upsilon(2S)$ decays without dipions in the final state, and $e^+e^- \rightarrow q\bar{q}$ events, we train an MLP using nine dipion kinematic variables [8]. The variables are: opening angle between the pions; absolute value of the cosine of the angle formed between the π^- and the direction of the $\Upsilon(2S)$ in the dipion frame; dipion momentum perpendicular to the beam axis; dipion invariant mass; distance from the beam spot; the larger momentum of the two pions; cosine of the dipion polar angle; χ^2 probability of the fit of the two pion tracks to a common vertex; and cosine of the polar angle of the more energetic pion. These quantities are calculated in the e^+e^- CM frame unless otherwise specified. Applying all other selection criteria, 99% of the remaining signal events and 80% of continuum events pass our MLP selection. The distribution of the recoil mass against the dipion system in data after applying all selection criteria is shown in Fig. 1.

We reconstruct $A^0 \rightarrow gg$ using 26 channels as listed in Table I. We do not use two-body decay channels

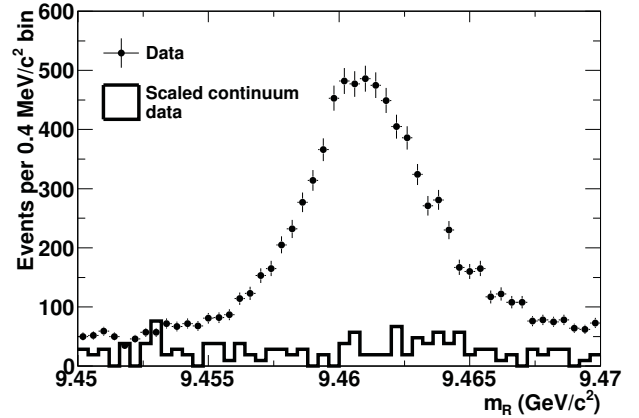


FIG. 1: Distribution of the recoil mass against the dipion system in on-resonance data (points with error bars) after applying all selection criteria. The histogram is the continuum background recoil mass distribution from off-resonance data normalized to the on-resonance integrated luminosity.

TABLE I: Decay modes for candidate $A^0 \rightarrow gg$ and $s\bar{s}$ decays, sorted by the total mass of the decay products.

#	Channel	#	Channel
1	$\pi^+\pi^-\pi^0$	14	$K^+K^-\pi^+\pi^-$
2	$\pi^+\pi^-2\pi^0$	15	$K^+K^-\pi^+\pi^-\pi^0$
3	$2\pi^+2\pi^-$	16	$K^\pm K_s^0 \pi^\mp \pi^\pm \pi^-$
4	$2\pi^+2\pi^-\pi^0$	17	$K^+K^-\eta$
5	$\pi^+\pi^-\eta$	18	$K^+K^-2\pi^+2\pi^-$
6	$2\pi^+2\pi^-2\pi^0$	19	$K^\pm K_s^0 \pi^\mp \pi^\pm \pi^- 2\pi^0$
7	$3\pi^+3\pi^-$	20	$K^+K^-2\pi^+2\pi^-\pi^0$
8	$2\pi^+2\pi^-\eta$	21	$K^+K^-2\pi^+2\pi^-2\pi^0$
9	$3\pi^+3\pi^-2\pi^0$	22	$K^\pm K_s^0 \pi^\mp 2\pi^+2\pi^-\pi^0$
10	$4\pi^+4\pi^-$	23	$K^+K^-3\pi^+3\pi^-$
11	$K^+K^-\pi^0$	24	$2K^+2K^-$
12	$K^\pm K_s^0 \pi^\mp$	25	$p\bar{p}\pi^0$
13	$K^+K^-2\pi^0$	26	$p\bar{p}\pi^+\pi^-$

because a CP -odd Higgs boson cannot decay into two pseudoscalar mesons. Charged kaons, pions, and protons are required to be positively identified. To reduce the number of misreconstructed candidates in an event, we require the number of reconstructed charged tracks in an event to match the number of charged tracks in the corresponding decay mode (including the $\pi^+\pi^-$). For example, we reconstruct ten-track events only as $K^+K^-3\pi^+3\pi^-$, $K^\pm K_s^0 \pi^\mp 2\pi^+2\pi^-\pi^0$ (two tracks from a K_s^0), or $4\pi^+4\pi^-$. The π^0 and η candidates are reconstructed from two photon candidates. The K_s^0 candidates are reconstructed using two charged pions of opposite charge. We define our $A^0 \rightarrow s\bar{s}$ sample as the subset of the 26 $A^0 \rightarrow gg$ decay channels that include two or four kaons (channels 11–24 in Table I). In simulated $A^0 \rightarrow s\bar{s}$ events, there is a negligible contribution from channels that do not include at least two kaons. We form an A^0 candidate by adding the four-momenta

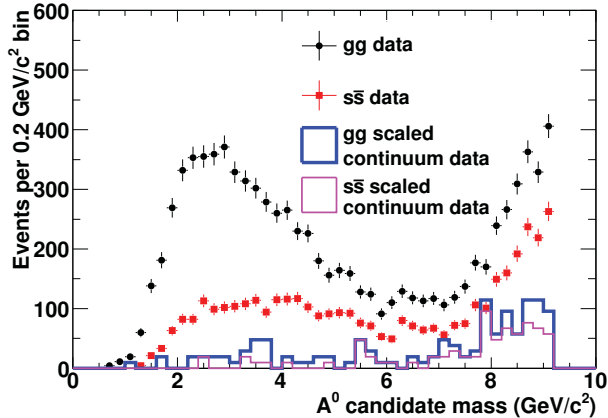


FIG. 2: A^0 candidate mass spectra after applying all selection criteria. We reconstruct $A^0 \rightarrow gg$ using the 26 channels listed in Table I and $A^0 \rightarrow s\bar{s}$ using the subset of the same 26 channels that includes two or four kaons. The A^0 candidate mass is the invariant mass of the reconstructed hadrons in each channel. The black points with error bars are on-resonance data for $A^0 \rightarrow gg$. The red squares with error bars are on-resonance data for $A^0 \rightarrow s\bar{s}$. The thick blue histogram is $A^0 \rightarrow gg$ in off-resonance data normalized to the on-resonance integrated luminosity. The thin magenta histogram is $A^0 \rightarrow s\bar{s}$ in off-resonance data normalized to the on-resonance integrated luminosity.

of the hadrons. Similarly, we form an $\Upsilon(1S)$ candidate by using the A^0 candidate and a photon with energy more than 200 MeV in the e^+e^- CM frame. To improve the A^0 mass resolution, we constrain the photon and the A^0 candidates to have an invariant mass equal to the $\Upsilon(1S)$ mass and a decay vertex at the beam spot. The χ^2 probability of the constrained fit is required to be greater than 10^{-3} . This rejects 77% of the misreconstructed A^0 candidates, which includes candidates with misidentified charged kaons, pions, and protons. We reject $\Upsilon(1S)$ candidates if the radiative photon, when combined with another photon in the event that is not used in the reconstruction of a π^0 or η candidate, has an invariant mass within 50 MeV/ c^2 of the π^0 mass. This removes backgrounds where a photon from a π^0 decay is misidentified as the radiative photon. We also reject $\Upsilon(1S)$ candidates if the Zernike moment A_{42} [19] of the radiative photon is greater than 0.1. This removes backgrounds where showers from both photons from a π^0 decay overlap and are mistaken as the radiative photon. If there is more than one $\Upsilon(2S) \rightarrow \pi^+\pi^-\Upsilon(1S)$, $\Upsilon(1S) \rightarrow \gamma A^0$ candidate that passes all the selection criteria in an event, the candidate with the highest product of MLP output and χ^2 probability is kept. Figure 2 shows the A^0 candidate invariant mass spectra for the $A^0 \rightarrow gg$ and $A^0 \rightarrow s\bar{s}$ channels separately after applying all selection criteria and selecting one candidate per event.

We use our off-resonance sample to estimate the continuum contribution in the on-resonance sample. Fifteen

percent of the candidates in the on-resonance sample are determined to come from non- $\Upsilon(2S)$ decays.

We use simulated $\Upsilon(2S)$ events to study the remaining backgrounds, which originate mainly from $\Upsilon(1S) \rightarrow ggg$ and $\Upsilon(1S) \rightarrow \gamma gg$, where the gluons hadronize to more than one daughter. In $\Upsilon(1S) \rightarrow ggg$ decays, a π^0 from the gluon hadronization is mistaken as the radiative photon. This decay mode contributes most of the background candidates with A^0 masses between 7 and 9 GeV/ c^2 . The candidates with A^0 masses between 2 and 4 GeV/ c^2 are mostly $\Upsilon(1S) \rightarrow \gamma gg$. CLEO measured the $\Upsilon(1S) \rightarrow \gamma f_2(1270)$ [20] and $\Upsilon(1S) \rightarrow \gamma f'_2(1525)$ [21] branching fractions. We do not expect these decays to be a background to the search for a narrow A^0 because they mainly decay to two-body final states and have decay widths of 100 MeV/ c^2 .

To determine the number of signal events, we define a mass window, centered on the hypothesis A^0 mass, that contains 80% of simulated signal events at that mass. For example, in simulated 3 GeV/ c^2 $A^0 \rightarrow s\bar{s}$ events, 80% of the events that pass the selection criteria have a reconstructed invariant mass for the A^0 within ± 170 MeV/ c^2 of 3 GeV/ c^2 . The mass windows are estimated for several A^0 masses for both gg and $s\bar{s}$, and interpolated for all other masses. A sideband region is defined as half of the mass window size adjacent to both sides of the mass window. Again, for example, the lower sideband for a 3 GeV/ c^2 $A^0 \rightarrow s\bar{s}$ would be from 2.66 to 2.83 GeV/ c^2 , and the upper sideband would be from 3.17 to 3.34 GeV/ c^2 .

Using simulated events, we estimate efficiencies of reconstructing the whole decay chain by taking the number of events in a signal mass window, subtracting the number of events in the sidebands, and dividing the difference by the number of simulated events. We interpolate the efficiencies for all hypothesis A^0 masses.

Our efficiency measurements of gg and $s\bar{s}$ into the 26 channels are dependent on the hadronization modelling by **Jetset**. The accuracies of the simulated branching fractions of gg and $s\bar{s}$ to different final states are difficult to determine. We correct for this by comparing simulations with data in $\Upsilon(1S) \rightarrow \gamma gg$ decays. We count the number of events in the 26 channels where the reconstructed gg mass is between 2 and 4 GeV/ c^2 in data, and compare that to simulated $\Upsilon(2S) \rightarrow \pi^+\pi^-\Upsilon(1S)$, $\Upsilon(1S) \rightarrow \gamma gg$ events in the same mass range. The background in this mass region is almost entirely from $\Upsilon(1S) \rightarrow \gamma gg$ decays. The number of $\Upsilon(1S) \rightarrow \gamma gg$ events is too few at masses above 4 GeV/ c^2 to allow any meaningful study. For each of the 26 channels listed in Table I, we calculate a weight that is the ratio of the event yields in data and simulation. We apply these weights to our efficiency calculations to determine how much the signal efficiency changes. The efficiencies change by a factor of 0.66 on average for $A^0 \rightarrow gg$ and 1.09 for $A^0 \rightarrow s\bar{s}$. We correct the efficiencies by multiplying our measured efficiencies by these factors and assign an uncertainty due to hadronization modelling of $(1 - 0.66)/0.66 = 50\%$ to all $A^0 \rightarrow gg$ and $A^0 \rightarrow s\bar{s}$

efficiencies since the correction is based on simulated $\Upsilon(1S) \rightarrow \gamma gg$ decays but not $\Upsilon(1S) \rightarrow \gamma s\bar{s}$ decays. We do not correct for, or assign hadronization modelling uncertainty to, $A^0 \rightarrow gg$ of invariant mass from 0.5 to 0.6 GeV/c^2 because a CP -odd A^0 can decay to only $\pi^+ \pi^- \pi^0$ in that mass region. Signal efficiencies range from 0.07 to 4×10^{-4} for gg and 0.04 to 1×10^{-3} for $s\bar{s}$. The efficiencies are lower for higher A^0 masses because a more massive A^0 decays to more hadrons, which increases the probability of misreconstruction.

An A^0 signal would appear as a narrow peak in the candidate mass spectrum. To look for a signal, we scan the mass spectrum in $10 \text{ MeV}/c^2$ steps from 0.5 GeV to $9.0 \text{ GeV}/c^2$. Our null hypothesis is that the signal rate is 0 in the signal mass window. We use sidebands to estimate the number of background events in the signal region. Using Cousins' method [22], we calculate a probability (p-value) of seeing the observed result or greater in the signal mass region given the null hypothesis. We do this separately for $A^0 \rightarrow gg$ and $A^0 \rightarrow s\bar{s}$. Figure 3 is the resulting p-value plot for all hypothesis masses. The minimum p-value for $A^0 \rightarrow gg$ is 0.003 and occurs at an A^0 mass of $8.13 \text{ GeV}/c^2$. The minimum p-value for $A^0 \rightarrow s\bar{s}$ is 0.002 and occurs at an A^0 mass of $8.63 \text{ GeV}/c^2$. These results are equivalent to Gaussian standard deviations of 2.7 and 2.9, respectively. We use 10^4 simulated experiments to calculate how often such a statistical fluctuation might occur. For $A^0 \rightarrow gg$, 86% of the simulated experiments have a minimum p-value less than 0.003. For $A^0 \rightarrow s\bar{s}$, 59% of the simulated experiments have a minimum p-value less than 0.002. Therefore, we conclude that there is no evidence for the light CP -odd Higgs boson.

The dominant systematic uncertainty on the product branching fraction upper limit is related to the efficiency, which was described earlier in the text. Other systematic uncertainties, which are small compared to the 50% uncertainty due to hadronization modelling, include Monte Carlo statistical uncertainties (1–7%), efficiency variations in estimating the size of the mass windows (5%), dipion branching fraction (2%), $\Upsilon(2S)$ counting (1%), and dipion selection efficiency (1%). The systematic uncertainties are summed in quadrature and total 51%.

We calculate 90%-confidence-level (CL) upper limits (Fig. 4) on the product branching fractions $\mathcal{B}(\Upsilon(1S) \rightarrow \gamma A^0) \cdot \mathcal{B}(A^0 \rightarrow gg)$ and $\mathcal{B}(\Upsilon(1S) \rightarrow \gamma A^0) \cdot \mathcal{B}(A^0 \rightarrow s\bar{s})$ using a profile likelihood approach [23]. We do this by calculating an upper limit of the mean number of signal events in the signal region given the number of events observed in the sidebands, and dividing by the efficiency, dipion branching fraction, and the number of $\Upsilon(2S)$ mesons produced. The number of background events is assumed to be Poissonian distributed and the efficiency distribution is assumed to be Gaussian with width equal to the total systematic uncertainty.

In summary, we select dipions in $\Upsilon(2S)$ decays to obtain a sample of $\Upsilon(1S)$ mesons. We reconstruct the $\Upsilon(1S)$ decay using a photon and a hadronic system. We

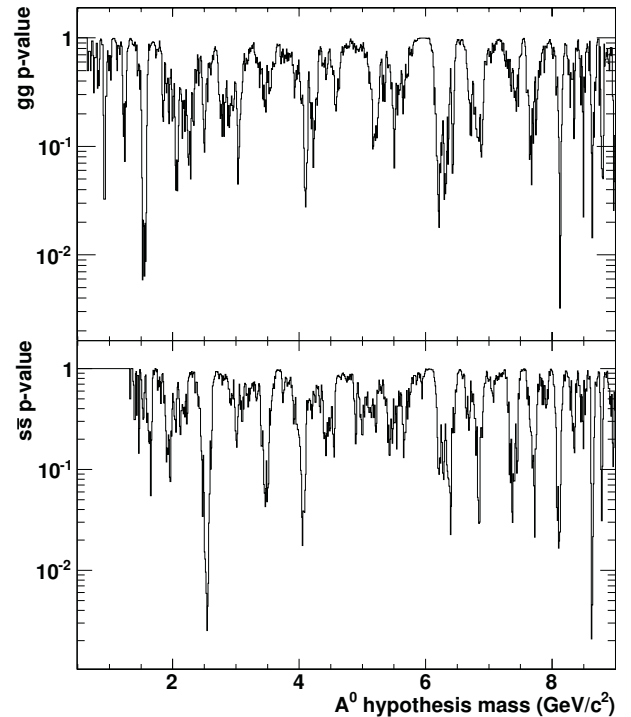


FIG. 3: The probability of observing at least the number of signal events, assuming a null hypothesis for the existence of the decay $\Upsilon(1S) \rightarrow \gamma A^0$, $A^0 \rightarrow gg$ (top), and $\Upsilon(1S) \rightarrow \gamma A^0$, $A^0 \rightarrow s\bar{s}$ (bottom).

observe no signals in the hadronic invariant mass spectra and set upper limits at 90% CL on the product branching fractions $\mathcal{B}(\Upsilon(1S) \rightarrow \gamma A^0) \cdot \mathcal{B}(A^0 \rightarrow gg)$ from 10^{-6} to 10^{-2} and $\mathcal{B}(\Upsilon(1S) \rightarrow \gamma A^0) \cdot \mathcal{B}(A^0 \rightarrow s\bar{s})$ from 10^{-5} to 10^{-3} . We do not observe a NMSSM A^0 or any narrow hadronic resonance.

We are grateful for the excellent luminosity and machine conditions provided by our PEP-II colleagues, and for the substantial dedicated effort from the computing organizations that support BABAR. The collaborating institutions wish to thank SLAC for its support and kind hospitality. This work is supported by DOE and NSF (USA), NSERC (Canada), IHEP (China), CEA and CNRS-IN2P3 (France), BMBF and DFG (Germany), INFN (Italy), FOM (The Netherlands), NFR (Norway), MIST (Russia), and PPARC (United Kingdom). Individuals have received support from CONACyT (Mexico), A. P. Sloan Foundation, Research Corporation, and Alexander von Humboldt Foundation.

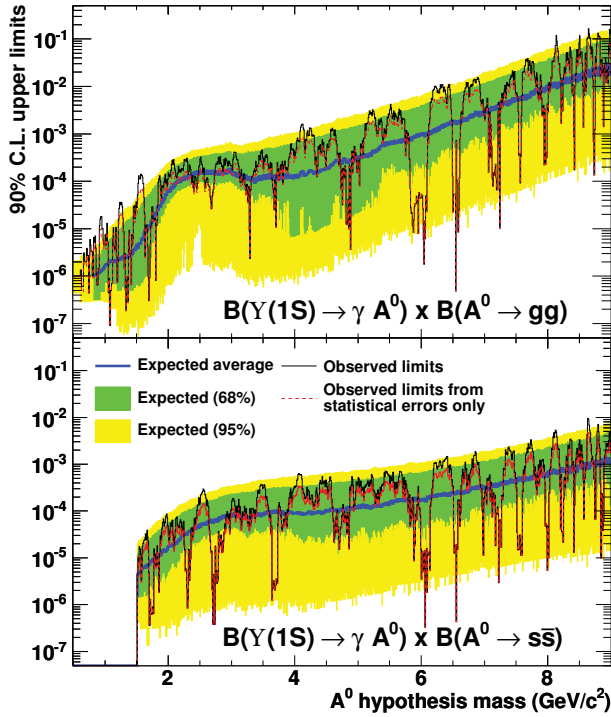


FIG. 4: (color online) The 90%-confidence-level upper limits (thin solid line) on the product branching fractions $\mathcal{B}(\Upsilon(1S) \rightarrow \gamma A^0) \cdot \mathcal{B}(A^0 \rightarrow gg)$ (top) and $\mathcal{B}(\Upsilon(1S) \rightarrow \gamma A^0) \cdot \mathcal{B}(A^0 \rightarrow s\bar{s})$ (bottom). We overlay limits calculated using statistical uncertainties only (thin dashed line). The inner band is the expected region of upper limits in 68% of simulated experiments. The inner band plus the outer band is the expected region of upper limits in 95% of simulated experiments. The bands are calculated using all uncertainties. The thick line in the center of the inner band is the expected upper limits calculated using simulated experiments.

-
- [1] M. Maniatis, *Int. J. Mod. Phys. A* **25**, 3505 (2010).
- [2] R. Dermisek, J. F. Gunion, and B. McElrath, *Phys. Rev. D* **76**, 051105(R) (2007).
- [3] R. Dermisek and J. F. Gunion, *Phys. Rev. D* **81**, 075003 (2010).
- [4] B. Aubert *et al.* (BABAR Collaboration), *Phys. Rev. Lett.* **103**, 081803 (2009).
- [5] J.P. Lees *et al.* (BABAR Collaboration), *Phys. Rev. D* **87**, 031102(R) (2013).
- [6] B. Aubert *et al.* (BABAR Collaboration), *Phys. Rev. Lett.* **103**, 181801 (2009).
- [7] J.P. Lees *et al.* (BABAR Collaboration), arXiv:1210.5669 [hep-ex] (2012), submitted to *Phys. Rev. D*.
- [8] P. del Amo Sanchez *et al.* (BABAR Collaboration), *Phys. Rev. Lett.* **107**, 021804 (2011).
- [9] J.P. Lees *et al.* (BABAR Collaboration), *Phys. Rev. Lett.* **107**, 221803 (2011).
- [10] S. Chatrchyan *et al.* (CMS Collaboration), *Phys. Rev. Lett.* **109**, 121801 (2012).
- [11] B. Aubert *et al.* (BABAR Collaboration), *Nucl. Instr. Methods Phys. Res. Sect. A* **479**, 1 (2002).
- [12] B. Aubert *et al.* (BABAR Collaboration), arXiv:1305.3560 [physics.ins-det] (2013), in press in *Nucl. Instr. Methods Phys. Res. Sect. A*.
- [13] J. P. Lees *et al.* (BABAR Collaboration), *Nucl. Instr. Methods Phys. Res. Sect. A* **726**, 203 (2013).
- [14] J. Beringer *et al.* (Particle Data Group), *Phys. Rev. D* **86**, 010001 (2012).
- [15] D. J. Lange, *Nucl. Instr. Methods Phys. Res. Sect. A* **462**, 152 (2001).
- [16] T. Sjöstrand, *Comp. Phys. Comm.* **82**, 74 (1994).
- [17] S. Agostinelli *et al.* (GEANT4 Collaboration), *Nucl. Instr. Methods Phys. Res. Sect. A* **506**, 250 (2003).
- [18] A. Höcker *et al.*, PoS ACAT, 040 (2007), arXiv:physics/0703039.
- [19] R. Sinkus and T. Voss, *Nucl. Instr. Methods Phys. Res. Sect. A* **391**, 360 (1997).
- [20] D. Besson *et al.* (CLEO Collaboration), *Phys. Rev. D* **75**, 072001 (2007).
- [21] D. Besson *et al.* (CLEO Collaboration), *Phys. Rev. D*

- 83**, 037101 (2011).
- [22] R. Cousins, J. Linnemann, and J. Tucker, Nucl. Instr. Methods Phys. Res. Sect. A **595**, 480 (2008).
- [23] W. Rolke *et al.*, Nucl. Instr. Methods Phys. Res. Sect. A **551**, 493 (2005).